

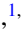




Enhanced spin-orbit coupling and orbital moment in ferromagnets by electron correlationsZe Liu ¹, Jing-Yang You ², Bo Gu ^{1,3,*}, Sadamichi Maekawa ^{4,1} and Gang Su ^{1,3,5,†}¹*Kavli Institute for Theoretical Sciences, and CAS Center for Excellence in Topological Quantum Computation, University of Chinese Academy of Sciences, Beijing 100190, China*²*Department of Physics, National University of Singapore, 2 Science Drive 3, Singapore 117551*³*Physical Science Laboratory, Huairou National Comprehensive Science Center, Beijing 101400, China*⁴*Center for Emergent Matter Science, RIKEN, Wako 351-0198, Japan*⁵*School of Physical Sciences, University of Chinese Academy of Sciences, Beijing 100049, China*

(Received 20 May 2021; revised 19 January 2023; accepted 30 January 2023; published 8 March 2023)

In atomic physics, the Hund's rule states that the largest spin and orbital state is realized due to the interplay of spin-orbit coupling (SOC) and Coulomb interactions. Here, we show that in ferromagnetic solids the effective SOC and the orbital magnetic moment can be dramatically enhanced by a factor of $1/[1 - (2U' - U - J_H)\rho_0]$, where U and U' are the on-site Coulomb interaction within the same orbitals and between different orbitals, respectively, J_H is the Hund's coupling, and ρ_0 is the average density of states. This factor is obtained by using the two-orbital as well as five-orbital Hubbard models with SOC. We also find that the spin polarization is more favorable than the orbital polarization, being consistent with experimental observations. The theory is also extended to study the spin fluctuations and long-range Coulomb interactions, and can be applied to understand the enhanced orbital magnetic moment and giant Faraday effect in ferromagnetic nanograins in recent experiments. This present paper provides a fundamental basis for understanding the enhancements of SOC and orbital moment by Coulomb interactions in ferromagnets, which would have wide applications in spintronics.

DOI: [10.1103/PhysRevB.107.104407](https://doi.org/10.1103/PhysRevB.107.104407)**I. INTRODUCTION**

The Hund's rule in atomic physics says that the state with both the largest spin moment and the largest orbital moment is realized in an atom, required by the minimum of the Coulomb repulsive energy. A similar picture was obtained in magnetic impurity systems. In the Anderson impurity model, the spin magnetic moment of impurities is developed due to a large on-site Coulomb interaction U [1]. In 1964, the extended Anderson impurity model with degenerate orbitals was studied, where the role of U and the Hund's coupling J_H was addressed [2,3]. Forty years ago, Yafet also studied the Anderson impurity model within the Hartree-Fock approximation and found that the on-site Coulomb interaction of impurities can enhance the effective spin-orbit coupling (SOC) in the spin-flip cross section [4]. Later, Fert and Jaoul applied this result to study the anomalous Hall effect due to magnetic impurities [5]. The relation between the on-site Coulomb interaction U and the effective SOC in magnetic impurity systems has also been discussed by density functional theory (DFT) calculations [6] and quantum Monte Carlo simulations [7]. The multiorbital Hubbard models have been extensively addressed by some advanced numerical calculations, such as quantum Monte Carlo simulations [8,9], and dynamical mean-field theory calculations [10–22]. The long-range Coulomb interactions in Hubbard models have also been studied [23–27].

In these years, one of the fast developing areas in condensed matter physics is spintronics [28,29]. It aims to manipulate the spin rather than the charge degree of freedom of electrons to design next-generation electronic devices of small size, with a faster calculating ability and lower energy consumption. SOC, as one of the key ingredients in spintronics, is related to many significant physical phenomena and novel matter [30]. In addition to the magnetic anisotropy [28,31], SOC plays an important role in phenomena such as the anomalous Hall effect [32,33], the spin Hall effect associated with the spin-charge conversion [34–37], topological insulators [38–42], skyrmions [43–45], and so on. To design better spintronic devices, a large SOC is usually required. As SOC is a relativistic effect in quantum mechanics, it is often small in many materials. A key issue is what factors can affect the magnitude of the SOC in solids.

On the other hand, the orbital moment in FeCo nanograins was experimentally shown to be about three times larger than that in bulk FeCo, as a result of the enhanced Coulomb interaction in the FeCo/insulator interface [46], because the Coulomb interaction in the FeCo/insulator interface is expected to be larger than that in the ferromagnetic FeCo bulk. In addition, a large Coulomb interaction up to 10 eV was discussed in Fe thin films in the experiment [47]. The spin polarization in the Hubbard model with Rashba SOC can also be enhanced by the on-site Coulomb interaction U [48]. Recently, in the two-dimensional magnetic topological insulators PdBr₃ and PtBr₃, DFT calculations show that the band gap and the SOC can be strongly enhanced by the Coulomb interaction [49]. The interplay of the Coulomb interaction and

*gubo@ucas.ac.cn

†gsu@ucas.ac.cn

spin-orbit coupling has been discussed by numerical calculations [50–55].

Inspired by recent experimental and numerical results on the enhanced SOC due to the Coulomb interaction in strongly correlated electronic systems, here we develop a theory on the relation between the SOC and Coulomb interaction in ferromagnets. By a two-orbital Hubbard model with SOC, we find that the effective SOC and orbital magnetic moment in ferromagnets can be enhanced by a factor of $1/[1 - (2U' - U - J_H)\rho_0]$, where U and U' are the on-site Coulomb interaction within the same orbitals and between different orbitals, respectively, J_H is the Hund's coupling, and ρ_0 is the average density of states. The same factor has also been obtained for a five-orbital Hubbard model with degenerate bands. Our theory can be viewed as the realization of Hund's rule in ferromagnets.

II. TWO-ORBITAL HUBBARD MODEL WITH SOC

Let us consider a two-orbital Hubbard model, where only a pair of orbitals with opposite orbital magnetic quantum numbers m (-1 and 1 , or -2 and 2) are considered. Thus, the Hamiltonian can be written as

$$H = \sum_{\mathbf{k}, m, \sigma} \epsilon_{\mathbf{k}m\sigma} n_{\mathbf{k}m\sigma} + U \sum_{i, m} n_{i, m\uparrow} n_{i, m\downarrow} + U' \sum_{i, \sigma, \sigma'} n_{i, m\sigma} n_{i, m'\sigma'} - J_H \sum_{i, \sigma} n_{i, m\sigma} n_{i, m\bar{\sigma}}, \quad (1)$$

where $\epsilon_{\mathbf{k}m\sigma}$ is the energy of an electron with wave vector \mathbf{k} , orbital m , and spin σ (\uparrow, \downarrow) [56], U and U' are the on-site Coulomb repulsion within the orbital m and between different orbitals m and m' , respectively, J_H is the Hund's coupling, and $n_{\mathbf{k}m\sigma}$ ($n_{i, m\sigma}$) represents the particle number with wave vector \mathbf{k} (site index i), orbital m , and spin σ . For simplicity, we consider four degenerate energy bands, which are lifted by an external magnetic field h and the Ising-type SOC [5],

$$\epsilon_{\mathbf{k}m\sigma} = \epsilon_{\mathbf{k}} - \sigma \mu_B h - \frac{1}{2} \sigma \lambda_{\text{so}} m, \quad (2)$$

where λ_{so} is the SOC constant, and $\epsilon_{\mathbf{k}}$ is the electron energy without an external magnetic field and SOC. Using the Hartree-Fock approximation, we have $n_{i, m\sigma} n_{i, m'\sigma'} \approx \langle n_{i, m\sigma} \rangle \langle n_{i, m'\sigma'} \rangle + \langle n_{i, m'\sigma'} \rangle \langle n_{i, m\sigma} \rangle - \langle n_{i, m\sigma} \rangle \langle n_{i, m'\sigma'} \rangle$. Assuming the system is homogeneous, the occupation number $n_{i, m\sigma}$ is independent of lattice site i , $\langle n_{i, m\sigma} \rangle \approx \langle n_{m\sigma} \rangle$, and through a Fourier transformation $\sum_i n_{i, m\sigma} = \sum_{\mathbf{k}} n_{\mathbf{k}m\sigma}$, the Hamiltonian in Eq. (1) can be diagonalized as

$$H \approx \sum_{\mathbf{k}, m, \sigma} \tilde{\epsilon}_{\mathbf{k}m\sigma} n_{\mathbf{k}m\sigma}, \quad (3)$$

with $\tilde{\epsilon}_{\mathbf{k}m\sigma} = \epsilon_{\mathbf{k}} - \sigma \mu_B h - \frac{1}{2} \sigma \lambda_{\text{so}} m + U \langle n_{m\bar{\sigma}} \rangle + U' (\langle n_{m\sigma} \rangle + \langle n_{m\bar{\sigma}} \rangle) - J_H \langle n_{m\bar{\sigma}} \rangle$. We define the spin polarization per site as $s_z = \mu_B (\langle n_{m\uparrow} \rangle - \langle n_{m\downarrow} \rangle) + \langle n_{m\uparrow} \rangle - \langle n_{m\downarrow} \rangle$, and the orbital polarization per site as $l_z = m \mu_B (\langle n_{m\uparrow} \rangle - \langle n_{m\downarrow} \rangle) + \langle n_{m\uparrow} \rangle - \langle n_{m\downarrow} \rangle$. Here, we should remark that the so-defined orbital polarization from itinerant electrons on different orbitals with SOC differs from the conventional orbital moments of atoms that are usually quenched owing to the presence of crystal fields in transition metal ferromagnets. We introduce the particle numbers of the parallel (n_p) and antiparallel (n_{ap})

states of the spin σ and orbital m : $n_p = \langle n_{m\uparrow} \rangle + \langle n_{m\downarrow} \rangle$, $n_{ap} = \langle n_{m\uparrow} \rangle - \langle n_{m\downarrow} \rangle$. Then the energy $\tilde{\epsilon}_{\mathbf{k}m\sigma}$ can be written as $\tilde{\epsilon}_{\mathbf{k}m\sigma} = \tilde{\epsilon} - \sigma \mu_B (h + \frac{U+J_H}{4\mu_B^2} s_z) - \frac{1}{2} m (\sigma \lambda_{\text{so}} - \frac{U-2U'+J_H}{2\mu_B m^2} l_z)$.

A. Spin polarization

It is noted that without an external magnetic field h and SOC λ_{so} , the four energy bands with spin σ (\uparrow and \downarrow) and orbital m (for example, 1 and -1) are degenerate, and the occupation numbers $n_{ap} = n_p$. In terms of the translational symmetry of the lattice system, $\langle n_{m\sigma} \rangle = \frac{1}{N} \sum_i \langle n_{i, m\sigma} \rangle = \frac{1}{N} \sum_{\mathbf{k}} \langle n_{\mathbf{k}m\sigma} \rangle = \frac{1}{N} \sum_{\mathbf{k}} f(\tilde{\epsilon}_{\mathbf{k}m\sigma})$, where f is the Fermi distribution function. For a system with a paramagnetic (PM) state ($h = 0$), $f(\tilde{\epsilon}_{\mathbf{k}m\sigma})$ can be expanded according to h , which is a small value compared to the Fermi energy, and $n_{ap} = n_p$, $s_z = \mu_B \sum_{\mathbf{k}} [f(\tilde{\epsilon}_{\text{PM}, km\uparrow}) - f(\tilde{\epsilon}_{\text{PM}, km\downarrow}) + f(\tilde{\epsilon}_{\text{PM}, k\bar{m}\uparrow}) - f(\tilde{\epsilon}_{\text{PM}, k\bar{m}\downarrow})] = 0$. Up to the linear order of h , the spin polarization becomes

$$s_z = \frac{4\mu_B^2 \rho_0}{1 - (U + J_H)\rho_0} h, \quad (4)$$

where $\rho_0 = \frac{1}{4} \int_0^\infty [-\frac{\partial f(E)}{\partial E}] [\rho_{m\uparrow}(E) + \rho_{m\downarrow}(E) + \rho_{m\downarrow}(E) + \rho_{\bar{m}\downarrow}(E)] dE$ is the average density of states of the four energy bands. The instability condition of the spin polarization is

$$(U + J_H)\rho_0 > 1. \quad (5)$$

This condition can be taken as an extension of the Stoner criterion in the presence of SOC in itinerant ferromagnets.

B. Orbital polarization

Similarly, the orbital polarization can be expressed as $l_z = \mu_B m (\langle n_{m\uparrow} \rangle - \langle n_{m\downarrow} \rangle + \langle n_{\bar{m}\uparrow} \rangle - \langle n_{\bar{m}\downarrow} \rangle) = \frac{\mu_B m}{N} \sum_{\mathbf{k}} [f(\tilde{\epsilon}_{\mathbf{k}m\uparrow}) - f(\tilde{\epsilon}_{\mathbf{k}m\downarrow}) + f(\tilde{\epsilon}_{\mathbf{k}\bar{m}\uparrow}) - f(\tilde{\epsilon}_{\mathbf{k}\bar{m}\downarrow})]$. For the ferromagnetic (FM) state, the SOC can be regarded as a small value [5], so $f(\tilde{\epsilon}_{\mathbf{k}m\sigma})$ can be expanded according to λ_{so} , and when $\lambda_{\text{so}} = 0$, $n_{ap} = n_p$, the zero-order term is zero. To the linear order of λ_{so} , the orbital polarization gives

$$l_z = \frac{m^2 \mu_B \rho_s}{1 - (2U' - U - J_H)\rho_0} \lambda_{\text{so}}, \quad (6)$$

where $\rho_s = \frac{1}{2} \int_0^\infty [-\frac{\partial f(E)}{\partial E}] [\rho_{m\uparrow}(E) + \rho_{m\downarrow}(E) - \rho_{m\downarrow}(E) - \rho_{\bar{m}\downarrow}(E)] dE$ is the average spin-polarized density of states. Then Eq. (6) can be rewritten as $l_z = \mu_B m^2 \rho_s \lambda_{\text{so}}^{\text{eff}}$, where the effective SOC $\lambda_{\text{so}}^{\text{eff}}$ is

$$\lambda_{\text{so}}^{\text{eff}} = \frac{\lambda_{\text{so}}}{1 - (2U' - U - J_H)\rho_0}. \quad (7)$$

One may note that the orbital polarization discussed here [Eq. (6)] is totally induced by the SOC, which can be enhanced by increasing U' or decreasing U and J_H ; we will discuss this in detail. In the absence of SOC, such an orbital polarization is absent according to Eq. (6). The instability condition of orbital polarization would be

$$(2U' - U - J_H)\rho_0 > 1. \quad (8)$$

The detailed derivation is given in the Supplemental Material [57].

TABLE I. Comparison of the theoretical results among the Anderson impurity model, the one-orbital Hubbard model (Stoner model), and our two- and five-orbital Hubbard models with spin-orbit coupling (SOC). s_z and l_z are the spin and orbital polarization, respectively. The instability conditions (ICs) of s_z and l_z in these models are listed. $\lambda_{\text{so}}^{\text{eff}}$ is the effective SOC affected by atomic SOC λ_{so} , the electron correlations U , U' , and J_H , and the electron density of states ρ . The equations of the five-orbital Hubbard model can be found in the Supplemental Material [57].

	Anderson impurity model	One-orbital Hubbard model (Stoner)	Two-orbital Hubbard SOC ($m = \pm 1$ or $m = \pm 2$)	Five-orbital Hubbard model with SOC ($m = 0, \pm 1, \pm 2$)
s_z		$\frac{2\mu_B^2 \rho(E_F)}{1-U\rho(E_F)} h$ [58]	$\frac{4\mu_B^2 \rho_0}{1-(U+J_H)\rho_0} h$ [Eq. (4)]	$\frac{10\mu_B^2 \rho_0}{1-(U+4J_H)\rho_0} h$ [Eq. (63)]
l_z			$\frac{m^2 \mu_B \rho_s}{1-(2U'-U-J_H)\rho_0} \lambda_{\text{so}}$ [Eq. (6)]	$\frac{\mu_B(\rho_{1s}+4\rho_{2s})}{1-(2U'-U-J_H)\rho_0} \lambda_{\text{so}}$ [Eq. (78)]
IC of s_z	$(U + 4J_H)\rho(E_F) > 1$ [2,3]	$U\rho(E_F) > 1$ [58]	$(U + J_H)\rho_0 > 1$ [Eq. (5)]	$(U + 4J_H)\rho_0 > 1$ [Eq. (65)]
IC of l_z			$(2U' - U - J_H)\rho_0 > 1$ [Eq. (8)]	
$\lambda_{\text{so}}^{\text{eff}}$	$\frac{\lambda_{\text{at}}}{1-(U-J_H)\rho(E_F)}$ [4]		$\frac{\lambda_{\text{so}}}{1-(2U'-U-J_H)\rho_0}$ [Eq. (7)]	

III. FIVE-ORBITAL HUBBARD MODEL WITH SOC

Our theory can be easily extended to the five-orbital Hubbard model with degenerate bands, and a detailed derivation is given in the Supplemental Material [57]. For the five-orbital case, the instability condition of the spin polarization becomes $(U + 4J_H)\rho_0 > 1$. The same expression has been obtained for the presence of a localized spin moment in the Anderson impurity model with degenerate orbitals [2,3]. The obtained instability condition of the orbital polarization is $(2U' - U - J_H)\rho_0 > 1$, which is the same as Eq. (8) for the two-orbital case. In the five-orbital case, the effective SOC and the orbital magnetic moment can also be enhanced by a factor of $1/[(2U' - U - J_H)\rho_0]$, that is, the same enhancement factor as in the two-orbital case.

IV. DISCUSSION

The comparison between our theory, the Stoner model, and the Anderson impurity model is shown in Table I. It is interesting to note that the instability conditions of s_z between our five-orbital Hubbard model with SOC and the Anderson impurity model are the same, while the obtained effective SOC $\lambda_{\text{so}}^{\text{eff}}$ between the two models are different. Comparing Eqs. (5) and (8), which are the spin and orbital instability conditions of the two-orbital model in Table I, one may note that the condition of spontaneous orbital polarization is more stringent than that of spontaneous spin polarization. The phase diagram of the spontaneous spin and orbital polarizations as a function of the inverse of average density of states $1/\rho_0$ and the Coulomb interaction U obtained with Eqs. (5) and (8) is depicted in Fig. 1. Considering the relation $U = U' + 2J_H$ and the reasonable values of $U = 4-7$ eV in the $3d$ transitional metal oxides [59], for $3d$ electrons, $J_H = 1$, $U' = 5$, $U = 7$ eV are a set of reasonable values, so for simplicity we keep the ratio $U : U' : J_H = 7 : 5 : 1$ in Eq. (7), and the shaded area with blue (red) solid lines indicates the spontaneous spin (orbital) polarization. The Stoner criterion of the spontaneous spin polarization based on the single-orbital Hubbard model is also plotted in Fig. 1 for comparison. The results show that the area of spontaneous orbital polarization is enclosed in an area of spontaneous spin polarization. In other words, it is more stringent to have spontaneous orbital polarization, which is

consistent with the fact that spontaneous orbital polarization is rarely observed in experiments.

In Stoner's theory, a single-orbital Hubbard model was studied with a mean-field approximation, and it is shown that the spin magnetic moment can be enhanced by a factor of $1/(1 - U\rho)$, the so-called Stoner enhancement factor. In our work, multiorbital Hubbard models are studied with a similar mean-field approximation, and it is shown that the orbital magnetic moments and the effective SOC can be enhanced by a factor of $1/[1 - (2U' - U - J_H)\rho_0]$. In both Stoner's theory and our work, the parameters of U , U' , and J_H are not so large, not in the large U values to induce the Mott metal-insulator transition.

V. EXTENSION OF OUR THEORY

We can extend our theory with the following three approaches. First, let us discuss the spin fluctuations in static

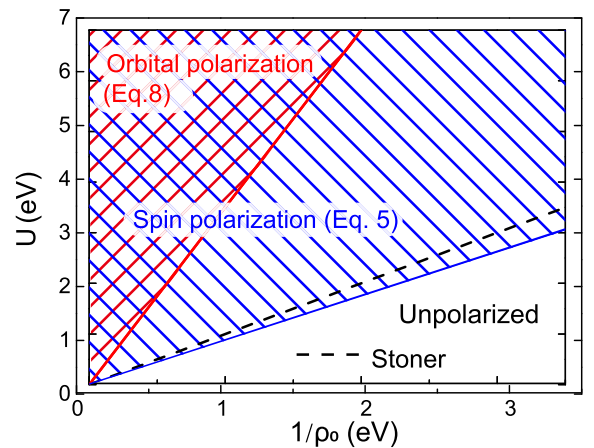


FIG. 1. The phase diagram of spontaneous spin and orbital polarizations as a function of the inverse average density of states and the Coulomb interaction U . The shaded area with blue solid lines represents the spontaneous spin polarization determined by Eq. (5). The shaded area with red solid lines represents the spontaneous orbital polarization determined by Eq. (8). The black dotted line indicates the Stoner criterion of the spontaneous spin polarization, which is obtained by the single-orbital Hubbard model.

magnetic susceptibility. In 1964, Hubbard had discussed the scattering correction and the resonance broadening correction in the single-orbital Hubbard model based on the higher-order Green's function [60]. Following Hubbard's paper, it is shown that there are three spin fluctuation terms appearing in the equation of motion. These spin fluctuation terms exactly cancel out each other, and do not appear in the final expression of the higher-order Green's function [60]. Although spin fluctuation terms can appear in even higher-order Green's functions, we note that the spin fluctuation in static magnetic susceptibility is a kind of higher-order effect, and could have small impacts on SOC. The details of the discussion are given in Sec. III of the Supplemental Material [57].

Second, we study the spin fluctuation and electron correlations in transverse dynamical susceptibility. By the random phase approximation, we calculated the transverse dynamical spin and orbital susceptibilities in a two-orbital Hubbard model. It is shown that transverse dynamic spin susceptibility can be enhanced by a factor of

$$\frac{1}{1 - U\Gamma_{\text{spin,m}}^{-+}(\mathbf{q}, \omega)}, \quad (9)$$

and the transverse dynamical orbital susceptibility can be enhanced by a factor of

$$\frac{1}{1 - (U' - J_H)\Gamma_{\text{orb},\sigma}^{-+}(\mathbf{q}, \omega)}, \quad (10)$$

where $\Gamma_{\text{spin,m}}^{-+}(\mathbf{q}, \omega)$ and $\Gamma_{\text{orb},\sigma}^{-+}(\mathbf{q}, \omega)$ are the transverse dynamic spin and orbital susceptibilities, respectively, without the Coulomb interactions. Our results show that the Coulomb interactions can enhance the transverse dynamical spin and orbital susceptibilities. The details are given in Sec. IV of the Supplemental Material [57].

Third, we consider the long-range Coulomb interactions and static magnetic susceptibility. With the Hartree-Fock approximation, we studied the effect of long-range Coulomb interactions in a five-orbital Hubbard model. We showed that the static spin susceptibility can be enhanced by a factor of

$$\frac{1}{1 - [U + 4J_H + (V - V'')Z]\rho_0}, \quad (11)$$

and the static orbital susceptibility and the effective SOC can be enhanced by a factor of

$$\frac{1}{1 - [2U' - U - J_H + (2V' - V - V'')Z]\rho_0}. \quad (12)$$

The long-range Coulomb interactions between the nearest-neighbor sites are considered: V between the same orbitals and different spins, V' between different orbitals and any spins, and V'' between the same orbitals and the same spins. Z is the number of nearest-neighbor sites. Our results reveal that the long-range Coulomb interactions can enhance the static magnetic susceptibility, the static orbital susceptibility, and the effective SOC. The details are given in Sec. V of the Supplemental Material [57].

VI. APPLICATIONS

Our theory can be applicable in the following two experiments: first, the large orbital magnetic moment in FeCo-MgF₂

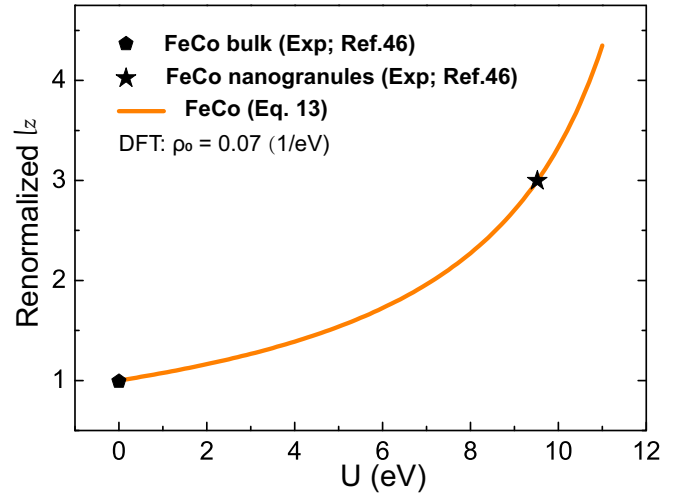


FIG. 2. The enhancement of orbital magnetic moment l_z in the FeCo nanogranules due to the Coulomb interaction U . The renormalized orbital moments of FeCo bulk and FeCo nanogranules in the experiment [46] are noted by the solid black pentagon and solid black star, respectively. The orange solid line is the result by Eq. (13), where ρ_0 is the density of states at the Fermi energy of the FeCo interface calculated by the DFT.

nanogranules in a recent experiment [46]. In the experiment, the orbital magnetic moment in FeCo nanogranules is observed to be three times larger than that of FeCo bulk. The orbital magnetic moment can be calculated by Eq. (6). The ratio of the orbital magnetic moment l_{z2} with the Coulomb interaction to the orbital magnetic moment l_{z1} without the Coulomb interaction can be approximately written as

$$\frac{l_{z2}}{l_{z1}} = \frac{1}{1 - (2U' - U - J_H)\rho_0}. \quad (13)$$

As shown in Fig. 2, substituting ρ_0 of the FeCo interface with $\rho_0 \sim 0.07$ (1/eV) obtained by DFT calculations and the ratio of $l_{z2}/l_{z1} = 3$ between the orbital magnetic moments of FeCo nanogranules and FeCo bulk in the experiment into Eq. (13), U can be estimated to be about 9.5 eV for the FeCo interface, which is somehow larger than the value of $U = 4-7$ eV used in the 3d transition metal compound [59]. Thus, Eq. (13) can be used to qualitatively explain the enhancement of orbital magnetic moment for the FeCo nanogranules in the experiment. The FeCo nanogranules can lead to enhanced Coulomb interactions due to the decreased screening effect at the FeCo/MgF₂ interface, and the enhanced Coulomb interactions at the interfaces can induce a large orbital magnetic moment.

The second is the giant Faraday effect in FeCo-(Al-fluoride) nanogranular films in a recent experiment [61]. In the experiment, the FeCo-(Al-fluoride) nanogranular films exhibiting Faraday rotation 40 times larger than that of Bi-YIG at the wavelength of the optical communication band. The effective SOC can be calculated by Eq. (7). The FeCo nanogranules can lead to the enhanced Coulomb interactions due to the decreased screening effect at the FeCo/Al-fluoride interface, where the enhanced Coulomb interactions at the interfaces can lead to the enhanced effective SOC, and the

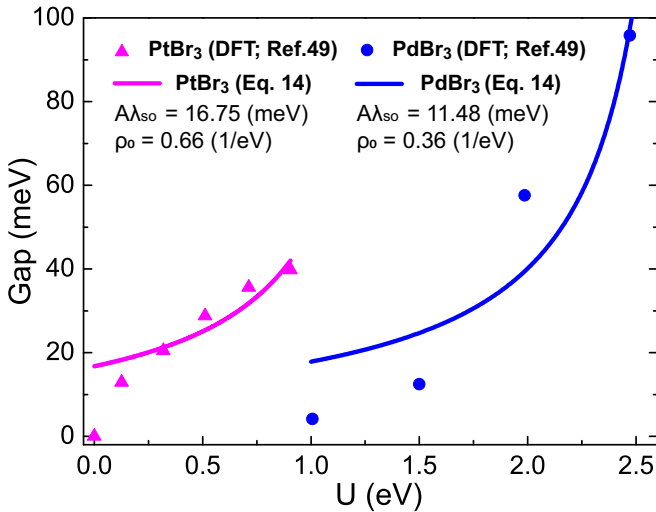


FIG. 3. The enhanced energy gap due to Coulomb interaction U . The blue solid triangles and purple solid circles give the band gap of PtBr₃ and PdBr₃, respectively, obtained by the density functional theory (DFT) calculations with different parameter U [49]. The blue and purple solid lines are fitted results by Eqs. (7) and (14), where the $A\lambda_{\text{so}}$ and ρ_0 are the fitting parameters.

latter can induce the enhanced Faraday effect. Similarly, the enhanced magneto-optical Kerr effect at the Fe/insulator interface was also predicted by numerical calculations [62].

Equation (7) shows that Coulomb interactions can enhance the effective SOC. Recently, for magnetic topological insulators PdBr₃ and PtBr₃, it is found that the energy gap increases with an increase of the Coulomb interaction U [49]. The enhancement of SOC by the Coulomb interaction U can be naturally obtained with Eq. (7). In these topological materials, the energy gap is opened due to the SOC, whereas the energy gap Δ_g can be approximately proportional to $\lambda_{\text{so}}^{\text{eff}}$,

$$\Delta_g = A\lambda_{\text{so}}^{\text{eff}}, \quad (14)$$

where A is the coefficient. As shown in Fig. 3, the blue solid triangles and purple solid circles represent the band gaps of PtBr₃ and PdBr₃, respectively, which are obtained by the DFT calculations with different U values [49]. The blue and purple solid lines are fitted by Eqs. (7) and (14), where $A\lambda_{\text{so}}$ and the density of state ρ_0 are the fitting parameters. For simplicity we use the approximation in the DFT calculation, to keep the $J_H = 0$ eV, $U = U'$ in Eq. (7), and study the effect of U in the $4d$ and $5d$ transition metal compounds. From Eqs. (7) and (14), it can be seen that the Coulomb interaction U can enhance the effective SOC parameter $\lambda_{\text{so}}^{\text{eff}}$, and thereby increase

the energy gap. Compared with numerical method such as DFT+ U , our paper gives the analytical equations that clearly show that electronic correlations can enhance the orbital moment and effective spin-orbital coupling in ferromagnets.

VII. CONCLUSION

Using a two-orbital Hubbard model with SOC, we show that the orbital polarization and the effective SOC in ferromagnets are enhanced by a factor of $1/[1 - (2U' - U - J_H)\rho_0]$, where U and U' are the on-site Coulomb interaction within the same orbitals and between different orbitals, respectively, J_H is the Hund's coupling, and ρ_0 is the average density of states. The same factor is obtained for the five-orbital Hubbard model with degenerate bands. Our theory can be viewed as the realization of Hund's rule in ferromagnets. The theory is also extended to study the spin fluctuation and long-range Coulomb interactions, and can be applied to understand the enhanced orbital magnetic moment and giant Faraday effect in ferromagnetic nanograins in recent experiments. In addition, our results reveal that it is more stringent to have spontaneous orbital polarization than spontaneous spin polarization, which is consistent with experimental observations. As the electronic interaction in some two-dimensional (2D) systems can be controlled experimentally [63], according to our theory, the enhanced SOC, spin, and orbital magnetic moments are highly expected to be observed in these 2D systems. This present work not only provides a fundamental basis for understanding the enhancements of SOC in some magnetic materials, but also sheds light on how to get a large SOC through hybrid spintronic structures.

ACKNOWLEDGMENTS

The authors acknowledge Q. B. Yan, Z. G. Zhu, and Z. C. Wang for many valuable discussions. This work is supported in part by the National Natural Science Foundation of China (Grants No. 12074378 and No. 11834014), the Beijing Natural Science Foundation (Grant No. Z190011), the National Key R&D Program of China (Grant No. 2018YFA0305800), the Beijing Municipal Science and Technology Commission (Grant No. Z191100007219013), the Chinese Academy of Sciences (Grants No. YSBR-030 and No. Y929013EA2), and the Strategic Priority Research Program of Chinese Academy of Sciences (Grants No. XDB28000000 and No. XDB33000000). S.M. is supported by JST CREST Grants (No. JPMJCR19J4, No. JPMJCR1874, and No. JPMJCR20C1) and JSPS KAKENHI (No. 17H02927 and No. 20H01865) from MEXT, Japan.

- [1] P. W. Anderson, Localized magnetic states in metals, *Phys. Rev.* **124**, 41 (1961).
- [2] T. Moriya, Ferro- and antiferromagnetism of transition metals and alloys, *Prog. Theor. Phys.* **33**, 157 (1965).
- [3] K. Yosida, A. Okiji, and S. Chikazumi, Magnetic anisotropy of localized state in metals, *Prog. Theor. Phys.* **33**, 559 (1965).

- [4] Y. Yafet, Spin-orbit induced spin-flip scattering by a local moment, *J. Appl. Phys.* **42**, 1564 (1971).
- [5] A. Fert and O. Jaoul, Left-Right Asymmetry in the Scattering of Electrons by Magnetic Impurities, and a Hall Effect, *Phys. Rev. Lett.* **28**, 303 (1972).
- [6] G. Y. Guo, S. Maekawa, and N. Nagaosa, Enhanced Spin Hall Effect by Resonant Skew Scattering in the

- Orbital-Dependent Kondo Effect, *Phys. Rev. Lett.* **102**, 036401 (2009).
- [7] B. Gu, J. Y. Gan, N. Bulut, T. Ziman, G. Y. Guo, N. Nagaosa, and S. Maekawa, Quantum Renormalization of the Spin Hall Effect, *Phys. Rev. Lett.* **105**, 086401 (2010).
- [8] J. E. Han, M. Jarrell, and D. L. Cox, Multiorbital Hubbard model in infinite dimensions: Quantum Monte Carlo calculation, *Phys. Rev. B* **58**, R4199 (1998).
- [9] S. Li, N. Kaushal, Y. Wang, Y. Tang, G. Alvarez, A. Nocera, T. A. Maier, E. Dagotto, and S. Johnston, Nonlocal correlations in the orbital selective Mott phase of a one-dimensional multi-orbital Hubbard model, *Phys. Rev. B* **94**, 235126 (2016).
- [10] A. Georges, G. Kotliar, W. Krauth, and M. J. Rozenberg, Dynamical mean-field theory of strongly correlated fermion systems and the limit of infinite dimensions, *Rev. Mod. Phys.* **68**, 13 (1996).
- [11] A. Liebsch, Single Mott transition in the multiorbital Hubbard model, *Phys. Rev. B* **70**, 165103 (2004).
- [12] A. Koga, N. Kawakami, T. M. Rice, and M. Sigrist, Orbital-Selective Mott Transitions in the Degenerate Hubbard Model, *Phys. Rev. Lett.* **92**, 216402 (2004).
- [13] T. Pruschke and R. Bulla, Hund's coupling and the metal-insulator transition in the two-band Hubbard model, *Eur. Phys. J. B* **44**, 217 (2005).
- [14] V. Drchal, V. Janiš, J. Kudrnovský, V. S. Oudovenko, X. Dai, K. Haule, and G. Kotliar, Dynamical correlations in multi-orbital Hubbard models: Fluctuation exchange approximations, *J. Phys.: Condens. Matter* **17**, 61 (2005).
- [15] K. Inaba, A. Koga, S. I. Suga, and N. Kawakami, Finite-temperature Mott transitions in the multiorbital Hubbard model, *Phys. Rev. B* **72**, 085112 (2005).
- [16] P. Werner and A. J. Millis, High-Spin to Low-Spin and Orbital Polarization Transitions in Multiorbital Mott Systems, *Phys. Rev. Lett.* **99**, 126405 (2007).
- [17] Y. Nomura, S. Sakai, and R. Arita, Nonlocal correlations induced by Hund's coupling: A cluster DMFT study, *Phys. Rev. B* **91**, 235107 (2015).
- [18] S. Hoshino and P. Werner, Electronic orders in multiorbital Hubbard models with lifted orbital degeneracy, *Phys. Rev. B* **93**, 155161 (2016).
- [19] K. Steiner, S. Hoshino, Y. Nomura, and P. Werner, Long-range orders and spin/orbital freezing in the two-band Hubbard model, *Phys. Rev. B* **94**, 075107 (2016).
- [20] A. J. Kim, H. O. Jeschke, P. Werner, and R. Valentí, J Freezing and Hund's Rules in Spin-Orbit-Coupled Multiorbital Hubbard Models, *Phys. Rev. Lett.* **118**, 086401 (2017).
- [21] P. Werner, H. U. R. Strand, S. Hoshino, Y. Murakami, and M. Eckstein, Enhanced pairing susceptibility in a photodoped two-orbital Hubbard model, *Phys. Rev. B* **97**, 165119 (2018).
- [22] A. J. Kim, P. Werner, and R. Valentí, Alleviating the sign problem in quantum Monte Carlo simulations of spin-orbit-coupled multiorbital Hubbard models, *Phys. Rev. B* **101**, 045108 (2020).
- [23] J. E. Hirsch, R. L. Sugar, D. J. Scalapino, and R. Blankenbecler, Monte Carlo simulations of one-dimensional fermion systems, *Phys. Rev. B* **26**, 5033 (1982).
- [24] J. E. Hirsch and D. J. Scalapino, $2p_F$ and $4p_F$ instabilities in a one-quarter-filled-band Hubbard model, *Phys. Rev. B* **27**, 7169 (1983).
- [25] R. Chitra and G. Kotliar, Effect of Long Range Coulomb Interactions on the Mott Transition, *Phys. Rev. Lett.* **84**, 3678 (2000).
- [26] A. Amaricci, A. Camjayi, K. Haule, G. Kotliar, D. Tanasković, and V. Dobrosavljević, Extended Hubbard model: Charge ordering and Wigner-Mott transition, *Phys. Rev. B* **82**, 155102 (2010).
- [27] L. Huang, T. Ayrál, S. Biermann, and P. Werner, Extended dynamical mean-field study of the Hubbard model with long-range interactions, *Phys. Rev. B* **90**, 195114 (2014).
- [28] I. Žutić, J. Fabian, and S. D. Sarma, Spintronics: Fundamentals and applications, *Rev. Mod. Phys.* **76**, 323 (2004).
- [29] *Concepts in Spin Electronics*, edited by S. Maekawa (Oxford University Press, New York, 2006).
- [30] A. Soumyanarayanan, N. Reyren, A. Fert, and C. Panagopoulos, Emergent phenomena induced by spin-orbit coupling at surfaces and interfaces, *Nature (London)* **539**, 509 (2016).
- [31] J. Y. You, Z. Zhang, X. J. Dong, B. Gu, and G. Su, Two-dimensional magnetic semiconductors with room Curie temperatures, *Phys. Rev. Res.* **2**, 013002 (2020).
- [32] N. Nagaosa, J. Sinova, S. Onoda, A. H. MacDonald, and N. P. Ong, Anomalous Hall effect, *Rev. Mod. Phys.* **82**, 1539 (2010).
- [33] J. Y. You, B. Gu, and G. Su, The p -orbital magnetic topological states on a square lattice, *Natl. Sci. Rev.* **9**, nwab114 (2022).
- [34] M. I. Dyakonov and V. I. Perel, Current-induced spin orientation of electrons in semiconductors, *Phys. Lett. A* **35**, 459 (1971).
- [35] J. E. Hirsch, Spin Hall Effect, *Phys. Rev. Lett.* **83**, 1834 (1999).
- [36] Y. K. Kato, R. C. Myers, A. C. Gossard, and D. D. Awschalom, Observation of the spin Hall effect in semiconductors, *Science* **306**, 1910 (2004).
- [37] J. Sinova, S. O. Valenzuela, J. Wunderlich, C. H. Back, and T. Jungwirth, Spin Hall effects, *Rev. Mod. Phys.* **87**, 1213 (2015).
- [38] L. Fu, C. L. Kane, and E. J. Mele, Topological Insulators in Three Dimensions, *Phys. Rev. Lett.* **98**, 106803 (2007).
- [39] J. E. Moore and L. Balents, Topological invariants of time-reversal-invariant band structures, *Phys. Rev. B* **75**, 121306(R) (2007).
- [40] M. Z. Hasan and C. L. Kane, Colloquium: Topological insulators, *Rev. Mod. Phys.* **82**, 3045 (2010).
- [41] X. L. Qi and S. C. Zhang, Topological insulators and superconductors, *Rev. Mod. Phys.* **83**, 1057 (2011).
- [42] J. Y. You, C. Chen, Z. Zhang, X. L. Sheng, S. A. Yang, and G. Su, Two-dimensional Weyl half-semimetal and tunable quantum anomalous Hall effect, *Phys. Rev. B* **100**, 064408 (2019).
- [43] S. Mühlbauer, B. Binz, F. Jonietz, C. Pfleiderer, A. Rosch, A. Neubauer, R. Georgii, and P. Boni, Skyrmion lattice in a chiral magnet, *Science* **323**, 915 (2009).
- [44] X. Z. Yu, Y. Onose, N. Kanazawa, J. H. Park, J. H. Han, Y. Matsui, N. Nagaosa, and Y. Tokura, Real-space observation of a two-dimensional skyrmion crystal, *Nature (London)* **465**, 901 (2010).
- [45] N. Nagaosa and Y. Tokura, Topological properties and dynamics of magnetic skyrmions, *Nat. Nanotechnol.* **8**, 899 (2013).
- [46] Y. Ogata, H. Chudo, B. Gu, N. Kobayashi, M. Ono, K. Harii, M. Matsuo, E. Saitoh, and S. Maekawa, Enhanced orbital magnetic moment in FeCo nanogranules observed by Barnett effect, *J. Magn. Magn. Mater.* **442**, 329 (2017).
- [47] R. Gotter, A. Verna, M. Sbroscia, R. Moroni, F. Bisio, S. Iacobucci, F. Offi, S. R. Vaidya, A. Ruocco, and G. Stefani, Unexpectedly Large Electron Correlation Measured in Auger Spectra of Ferromagnetic Iron Thin Films: Orbital-Selected

- Coulomb and Exchange Contributions, *Phys. Rev. Lett.* **125**, 067202 (2020).
- [48] J. A. Riera, Spin polarization in the Hubbard model with Rashba spin-orbit coupling on a ladder, *Phys. Rev. B* **88**, 045102 (2013).
- [49] J. Y. You, Z. Zhang, B. Gu, and G. Su, Two-Dimensional Room-Temperature Ferromagnetic Semiconductors with Quantum Anomalous Hall Effect, *Phys. Rev. Appl.* **12**, 024063 (2019).
- [50] M. Kim, J. Mravlje, M. Ferrero, O. Parcollet, and A. Georges, Spin-Orbit Coupling and Electronic Correlations in Sr_2RuO_4 , *Phys. Rev. Lett.* **120**, 126401 (2018).
- [51] J. Bünemann, T. Linneweber, U. Löw, F. B. Anders, and F. Gebhard, Interplay of Coulomb interaction and spin-orbit coupling, *Phys. Rev. B* **94**, 035116 (2016).
- [52] R. Triebl, G. J. Kraberger, J. Mravlje, and M. Aichhorn, Spin-orbit coupling and correlations in three-orbital systems, *Phys. Rev. B* **98**, 205128 (2018).
- [53] N.-O. Linden, M. Zingl, C. Hubig, O. Parcollet, and U. Schollwöck, Imaginary-time matrix product state impurity solver in a real material calculation: Spin-orbit coupling in Sr_2RuO_4 , *Phys. Rev. B* **101**, 041101(R) (2020).
- [54] X. Cao, Y. Lu, P. Hansmann, and M. W. Haverkort, Tree tensor-network real-time multiorbital impurity solver: Spin-orbit coupling and correlation functions in Sr_2RuO_4 , *Phys. Rev. B* **104**, 115119 (2021).
- [55] M. Richter, J. Graspentner, T. Schäfer, N. Wentzell, and M. Aichhorn, Comparing the effective enhancement of local and nonlocal spin-orbit couplings on honeycomb lattices due to strong electronic correlations, *Phys. Rev. B* **104**, 195107 (2021).
- [56] T. A. Kaplan, Single-band Hubbard model with spin-orbit coupling, *Z. Phys. B* **49**, 313 (1983).
- [57] See Supplemental Material at <http://link.aps.org/supplemental/10.1103/PhysRevB.107.104407> for details of the derivation process for analytical equations that electronic correlations can enhance the orbital moment and effective spin-orbital coupling, and extension of our theory, which includes Refs. [5,60].
- [58] E. C. Stoner, Collective electron ferromagnetism, *Proc. R. Soc. London, Ser. A* **165**, 372 (1938).
- [59] S. Maekawa, T. Tohyama, S. E. Barnes, S. Ishihara, W. Koshibae, and G. Khaliullin, *Physics of Transition Metal Oxides* (Springer, New York, 2004).
- [60] J. Hubbard, Electron correlations in narrow energy bands. III. An improved solution, *Proc. R. Soc. London, Ser. A* **281**, 401 (1964).
- [61] N. Kobayashi, K. Ikeda, B. Gu, S. Takahashi, H. Masumoto, and S. Maekawa, Giant Faraday rotation in metal-fluoride nanogranular films, *Sci. Rep.* **8**, 4978 (2018).
- [62] B. Gu, S. Takahashi, and S. Maekawa, Enhanced magneto-optical Kerr effect at Fe/insulator interfaces, *Phys. Rev. B* **96**, 214423 (2017).
- [63] X. Liu, Z. Wang, K. Watanabe, T. Taniguchi, O. Vafek, and J. I. A. Li, Tuning electron correlation in magic-angle twisted bilayer graphene using Coulomb screening, *Science* **371**, 1261 (2021).